AD-A175 661 LOWTRAN MODELING OF NEAR-HORIZON INFRARED SKY RADIANCES 1/1
IN THE PRESENCE OF CLOUDS(U) NAVAL OCEAN SYSTEMS CENTER
SAN DIEGO CA H G HUGHES SEP 86 NOSC/TD-988

UNCLASSIFIED F/G 17/5 NL

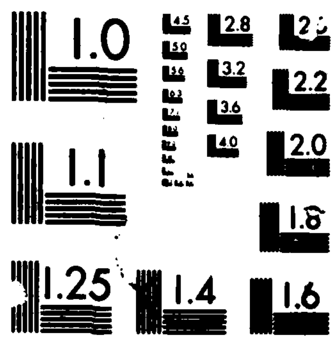
1.0
1.1
1.25
1.4
1.6
1.8
2.0
2.2
2.8
3.2
3.6
4.0

NOSC TD 988

AD-A175 661

NOSC

NAVAL OCEAN SYSTEMS CENTER San Diego, California 92152-5000

(12)

Technical Document 988
September 1986

LOWTRAN Modeling of Near-Horizon Infrared Sky Radiances in the Presence of Clouds

H. G. Hughes

Approved for public release; distribution is unlimited.

NAVAL OCEAN SYSTEMS CENTER

San Diego, California 92152-5000

F. M. PESTORIUS, CAPT, USN
Commander

R. M. HILLYER
Technical Director

ADMINISTRATIVE INFORMATION

The work reported herein was sponsored by the Naval Air Systems Command over the period October 1985 to September 1986. Additional support was provided by the Naval Sea Systems Command under Program Element 63221C.

Released by
H. V. Hitney, Head
Tropospheric Branch

Under the authority of
J. H. Richter, Head
Ocean and Atmospheric
Sciences Division

ACKNOWLEDGMENTS

Appreciation is extended to William J. Schade, who made available the radiance measurements, and to David B. Law for his assistance with the LOWTRAN calculations. The radiosonde measurements aboard the USS *Point Loma* (AGDS-2) were provided by a Mobile Environmental Team directed by LT Greg A. Elsman of the Naval Oceanographic Command Facility, San Diego, CA. Programs for processing the radiosonde data were provided by Richard A. Paulus. Douglas E. Chevrier of the Pacific Missile Test Center, Pt. Mugu, CA, was responsible for the shipboard radon measurements.

UNCLASSIFIED
SECURITY CLASSIFICATION OF THIS PAGE

ADA175661

REPORT DOCUMENTATION PAGE

1a. REPORT SECURITY CLASSIFICATION: UNCLASSIFIED	1b. RESTRICTIVE MARKINGS
2a. SECURITY CLASSIFICATION AUTHORITY	3. DISTRIBUTION/AVAILABILITY OF REPORT: Approved for public release; distribution is unlimited.
2b. DECLASSIFICATION/DOWNGRADING SCHEDULE	
4. PERFORMING ORGANIZATION REPORT NUMBER(S): NOSC TD 988	5. MONITORING ORGANIZATION REPORT NUMBER(S)
6a. NAME OF PERFORMING ORGANIZATION: Naval Ocean Systems Center; 6b. OFFICE SYMBOL (if applicable): Code 543	7a. NAME OF MONITORING ORGANIZATION
6c. ADDRESS (City, State and ZIP Code): San Diego, CA 92152-5000	7b. ADDRESS (City, State and ZIP Code)
8a. NAME OF FUNDING/SPONSORING ORGANIZATION: Naval Air Systems Command; 8b. OFFICE SYMBOL (if applicable): NAIR-330	9. PROCUREMENT INSTRUMENT IDENTIFICATION NUMBER
8c. ADDRESS (City, State and ZIP Code): Washington, DC 20361	10. SOURCE OF FUNDING NUMBERS

PROGRAM ELEMENT NO.	PROJECT NO.	TASK NO.	AGENCY ACCESSION NO.
61153N	WR03302		DN213 055

11. TITLE (include Security Classification)

LOWTRAN Modeling of Near-Horizon Infrared Sky Radiances in the Presence of Clouds

12. PERSONAL AUTHOR(S)

H.G. Hughes

13a. TYPE OF REPORT	13b. TIME COVERED	14. DATE OF REPORT (Year, Month, Day)	15. PAGE COUNT
Research	FROM Oct 1985 TO Sep 1986	September 1986	17

16. SUPPLEMENTARY NOTATION

17. COSATI CODES

FIELD	GROUP	SUB-GROUP

18. SUBJECT TERMS (Continue on reverse if necessary and identify by block number)

Optical scattering
Atmospheric modeling
Aerosol size distribution
Radiance algorithm
Infrared radiance
Thermal imaging

19. ABSTRACT (Continue on reverse if necessary and identify by block number)

A set of infrared (8 — 12 μm) sky radiances and meteorological (radiosonde) measurements are used to test the utility of the LOWTRAN 6 radiance algorithm to predict infrared sky radiances close to the horizon when clouds are present. The effects of clouds on the calculated radiances at the optical horizon are shown to be minimal but must be properly included at slightly higher elevations. Although the measurements pertain to good surface visibility conditions, small contributions by aerosols must be included in the LOWTRAN 6 calculations in order to match the measured radiances. This points out the possibility of inferring an appropriate (but not unique) vertical aerosol size distribution model from remotely sensed sky radiances. A deficiency in the radiance algorithm at a zenith angle of 90° was noted, and its sensitivity to the number of lower layers used in the atmospheric model is discussed.

20. DISTRIBUTION/AVAILABILITY OF ABSTRACT: [x] UNCLASSIFIED/UNLIMITED [ ] SAME AS RPT [ ] DTIC USERS	21. ABSTRACT SECURITY CLASSIFICATION: UNCLASSIFIED
22a. NAME OF RESPONSIBLE INDIVIDUAL: H.G. Hughes	22b. TELEPHONE (include Area Code): (619) 225-6520; 22c. OFFICE SYMBOL: Code 543

DD FORM 1473, 84 JAN

83 APR EDITION MAY BE USED UNTIL EXHAUSTED
ALL OTHER EDITIONS ARE OBSOLETE

UNCLASSIFIED
SECURITY CLASSIFICATION OF THIS PAGE

INTRODUCTION

The primary factors affecting infrared electrooptical surveillance, guidance, and weapons systems in the marine environment are atmospheric water vapor and aerosols, which absorb and scatter the radiation. In the absence of real-time measurements, we must presently rely on the atmospheric propagation code LOWTRAN 6 (Kneizys et al., 1983) to predict infrared transmission losses and sky backgrounds, using as inputs measured meteorological parameters. The effects of water vapor absorptions are readily handled by LOWTRAN 6. However, the existing models of aerosol size distributions are based on surface meteorological parameters,and the models' variations with altitude (humidity or visibility variations) are as yet unproven. Further, the effects of clouds on the LOWTRAN predictions have not been examined. In this report, a set of infrared (8–12 μm) sky radiances and meteorological parameters are used to investigate the utility of the LOWTRAN 6 radiance algorithm to predict infrared sky radiances close to the horizon when clouds are present.

MEASUREMENTS

For these investigations, a set of infrared (8–12 μm) sky radiances were obtained during the diurnal period from 1945 PST, 15 April 1986 to 1645 PST, 16 April 1986. Radiance measurements close to the horizon were obtained with a calibrated thermal imaging system (AGA THERMOVISION, Model 780) with a lens of 3.5° FOV and IFOV of 0.9 mrad. The response of each wavelength band is determined by placing a blackbody of known temperature ($\pm$ 0.1°C for temperatures $<$ 50°C) close to the aperture of the lens. The digitized video signal transfer function of the system then allows the blackbody temperature to be reproduced to within $\pm$ 0.2°C. The video output of the scanner is digitized and processed on a microcomputer to allow the temperature of selected pixels of the scene to be displayed. For these measurements the scanner was directed due west over the ocean from an altitude of 33 m such that approximately 2° of the FOV was above the horizon. During the recording period four radiosondes were launched from a ship (USS *Point Loma* (AGDS-2)) 5 km off the coast of Pt. Loma, San Diego, CA. The radiosonde system employed was the VAISALA model RS80. The measured temperature and relative humidity variations with altitude for the four periods (1945 PST, 15 April; 0845, 1245, 1645 PST, 16 April) are shown graphically in Fig. 1 and tabulated with the pressure variations in Table 1. During the first launch the sky was overcast by a stratus layer approximately 300 m thick with its base near 900 m altitude. During the subsequent launches, the clouds persisted,but the coverage was either broken (second launch) or scattered (third and fourth launches). Visibility measurements were not available; however, offshore islands about 35 km distant were clearly seen. Surface wind speeds and directions were recorded continuously on shore at the sensor site and periodically aboard the ship. The wind was predominantly northwesterly (310° $\pm$ 10°) throughout the measurements, with speeds varying as shown in Fig. 2. Measurements of atmospheric radon were also made aboard the USS *Point Loma* to aid in determining the air mass characteristics. The radon counts measured as a function of time are shown in Fig. 3 and indicate the air mass was primarily of maritime origin ($<$4 pCi/m^3) throughout the measurement period. The increased radon counts near 0400 PST on 15 April coincide with the in-port time of the ship.

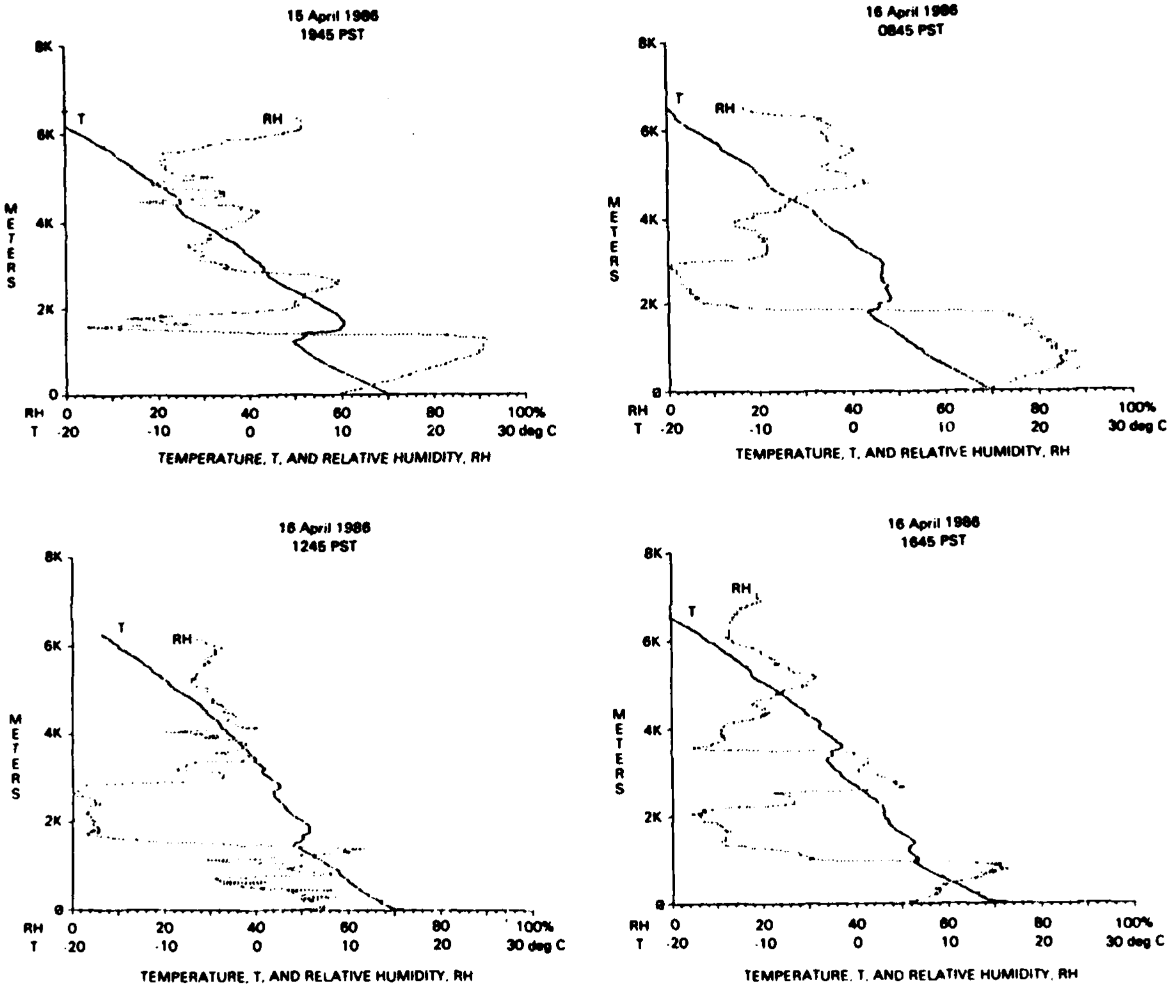

Figure 1. Radiosonde measurements of temperature and relative humidity variations with altitude.

Table 1. Radiosonde measurements of pressure (p, mb) temperature (T, °K), and relative humidity (REL H, %) with altitude (Z,km).

15 April 1986, 1945 PST

Z (KM)	P (MB)	T (K)	REL H (%)
.008	1015.800	288.05	60.00
.143	999.700	287.05	64.00
.263	985.500	285.75	68.00
.383	971.600	284.55	72.00
.501	957.800	283.25	75.00
.575	949.300	282.65	78.00
.738	930.900	281.25	84.00
.870	916.100	280.15	87.00
.901	912.900	279.95	89.00
1.016	900.000	279.15	91.00
1.238	876.200	278.35	91.00
1.369	862.300	279.15	51.00
1.560	842.600	283.45	5.00
1.648	833.600	283.45	25.00
1.767	821.800	283.25	15.00
1.988	800.200	281.65	49.00
2.296	770.800	278.85	52.00
2.514	750.500	276.95	58.00
2.644	738.600	275.95	59.00
2.759	728.100	275.35	55.00
2.932	712.700	274.85	35.00
3.075	700.100	274.15	32.00
3.503	663.700	272.15	29.00
4.247	604.000	265.75	41.00
4.344	596.500	265.45	39.00
4.455	588.000	265.75	18.00
4.565	579.700	265.55	34.00
4.676	571.500	264.45	34.00
4.841	559.400	263.25	20.00
5.006	547.600	262.15	31.00
5.101	540.800	261.45	23.00
5.535	510.900	258.45	21.00
5.697	500.100	257.45	29.00

16 April 1986, 0845 PST

Z (KM)	P (MB)	T (K)	REL H (%)
.008	1014.800	288.55	65.00
.068	1007.600	287.55	70.00
.143	998.700	286.85	73.00
.218	989.800	286.25	75.00
.308	979.300	285.45	78.00
.428	965.400	284.45	81.00
.532	953.500	283.45	84.00
.650	940.000	282.45	86.00
.783	925.100	281.45	86.00
.843	918.500	280.95	86.00
.901	912.000	280.75	86.00
1.018	899.100	280.15	84.00
1.123	889.500	279.45	83.00
1.225	878.500	278.75	81.00
1.356	864.500	277.95	80.00
1.458	853.800	277.15	78.00
1.544	844.800	276.45	78.00
1.629	834.300	275.85	78.00
1.773	819.600	274.95	72.00
1.903	806.500	276.15	15.00
2.047	792.300	277.35	8.00
2.957	708.200	276.65	2.00
3.087	697.000	275.45	20.00
3.658	649.100	271.85	21.00
3.899	629.700	270.25	16.00
4.292	599.100	268.05	25.00
4.612	575.000	265.05	33.00
4.778	562.900	264.25	43.00
5.149	536.500	262.75	35.00
5.531	510.400	259.45	40.00

16 April 1986, 1245 PST

Z (KM)	P (MB)	T (K)	REL H (%)
.008	1017.700	288.65	50.00
.083	1008.700	287.55	54.00
.158	999.700	286.75	54.00
.233	990.900	286.25	[illegible]
.264	987.400	286.05	[illegible]
.338	978.600	285.25	50.00
.457	964.800	284.35	[illegible]
.590	949.400	283.35	35.00
.650	942.700	283.25	31.00
.724	934.300	282.75	36.00
.798	926.100	282.45	57.00
.856	911.500	282.05	49.00
.931	911.300	281.75	48.00
.960	908.100	281.55	49.00
1.034	900.000	280.75	48.00
1.122	890.500	280.25	32.00
1.384	862.400	278.15	63.00
1.515	848.700	277.75	23.00
1.689	830.700	278.45	4.00
2.412	760.000	275.95	5.00
2.700	733.400	275.15	1.00
2.843	720.400	275.65	4.00
2.930	712.800	274.95	32.00
3.102	697.700	273.85	32.00
3.159	692.800	273.95	24.00
3.330	678.100	273.35	26.00
3.459	667.300	272.85	39.00
3.729	645.100	271.45	37.00
4.040	620.400	270.05	26.00
4.152	611.600	269.35	36.00
5.085	542.800	264.05	27.00
5.687	501.900	260.25	28.00

16 April 1986, 1645 PST

Z (KM)	P (MB)	T (K)	REL H (%)
.008	1016.100	288.85	50.00
.083	1007.100	287.25	54.00
.143	999.900	286.55	56.00
.233	989.300	285.75	58.00
.308	980.600	285.25	58.00
.413	968.400	284.25	60.00
.427	966.700	284.05	58.00
.575	949.600	282.55	66.00
.722	932.900	281.25	71.00
.738	931.200	281.05	71.00
.869	916.400	279.95	71.00
.885	914.800	279.75	71.00
.957	906.700	279.45	54.00
.987	903.400	279.75	31.00
1.015	900.200	279.75	30.00
1.177	882.800	278.95	28.00
1.323	867.200	279.25	13.00
1.483	850.400	279.15	11.00
1.860	811.900	276.75	9.00
2.062	791.900	276.25	6.00
2.292	769.700	275.65	26.00
2.422	757.400	274.85	26.00
2.522	748.000	274.15	23.00
2.622	738.800	273.45	50.00
2.964	707.900	271.65	41.00
3.261	681.900	270.15	42.00
3.444	666.300	270.65	40.00
3.558	656.900	271.85	7.00
4.094	613.900	269.55	11.00
4.569	577.800	266.75	18.00
5.149	536.200	262.45	32.00
5.286	526.700	262.05	26.00
5.653	502.000	259.75	21.00

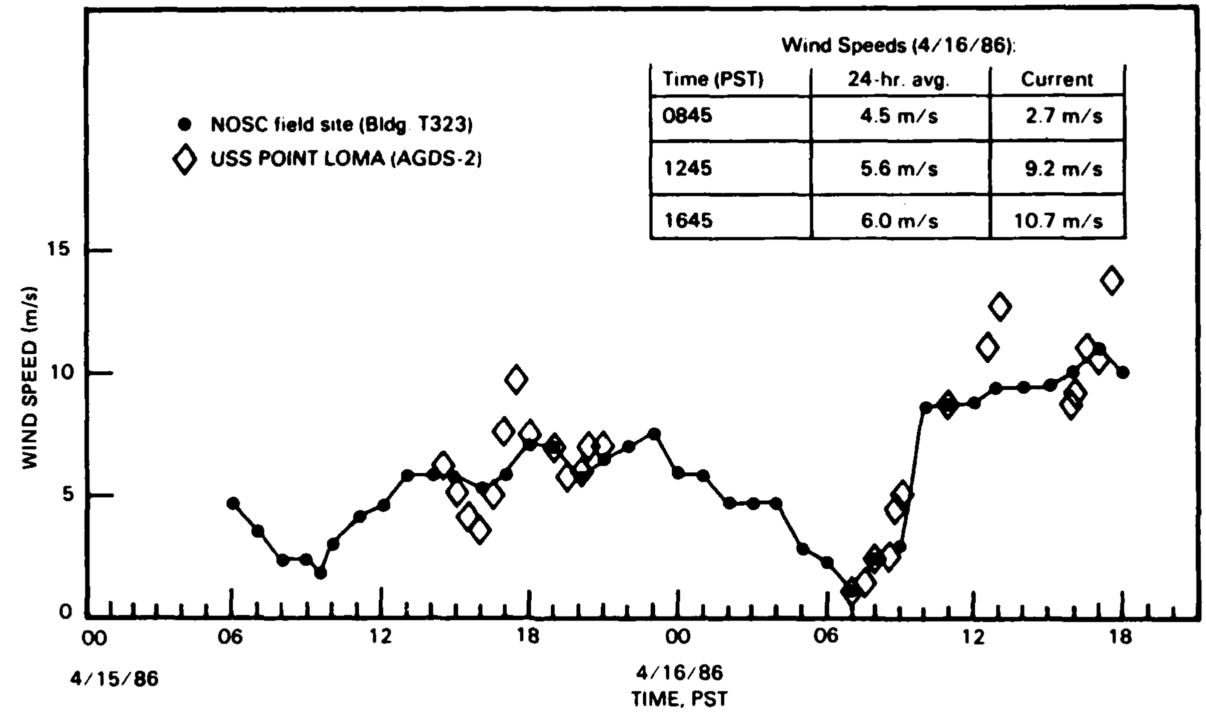

Figure 2. Surface wind speed variations with time of day.

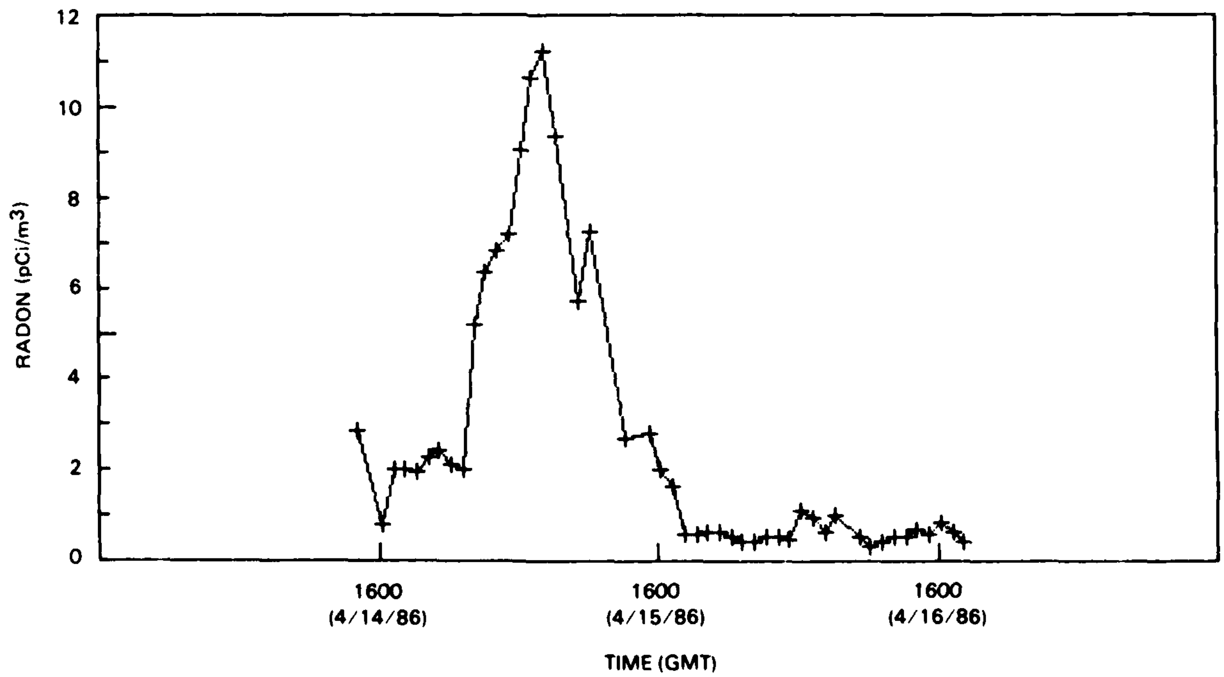

Figure 3. Measurements of radon counts at sea with time of day.

COMPARISON OF MEASUREMENTS AND CALCULATIONS

In Fig. 4 the sky radiances measured with zenith angle are compared to those calculated with the LOWTRAN 6 code by means of the radiosonde data of the first launch, when the sky was overcast. The AGA system's viewing angle was not plumbed to the zenith, with the result that the zenith angle of the optical horizon could not be accurately measured. For the purpose of these comparisons the maximum radiance at the sea–sky interface in the thermogram was taken to coincide with the optical horizon as calculated by the LOWTRAN code for the existing meteorological conditions. The details of the measurements and radiance values utilized here have been presented elsewhere by Schade and Law (1986). The clear-air calculations (without aerosols) were made using a nine-layer atmospheric model below the 901-m cloud base provided by the radiosonde data, and assuming the cloud base to be a blackbody radiator at the measured ambient temperature of 6.8°C. Whether or not the cloud was indeed "black" can not be determined. However, for stratus clouds of this thickness (337 m), liquid water paths exceeding the required 30 gm/m^3 (Stephens, 1978) for the cloud emissivity to approach unity are not uncommon

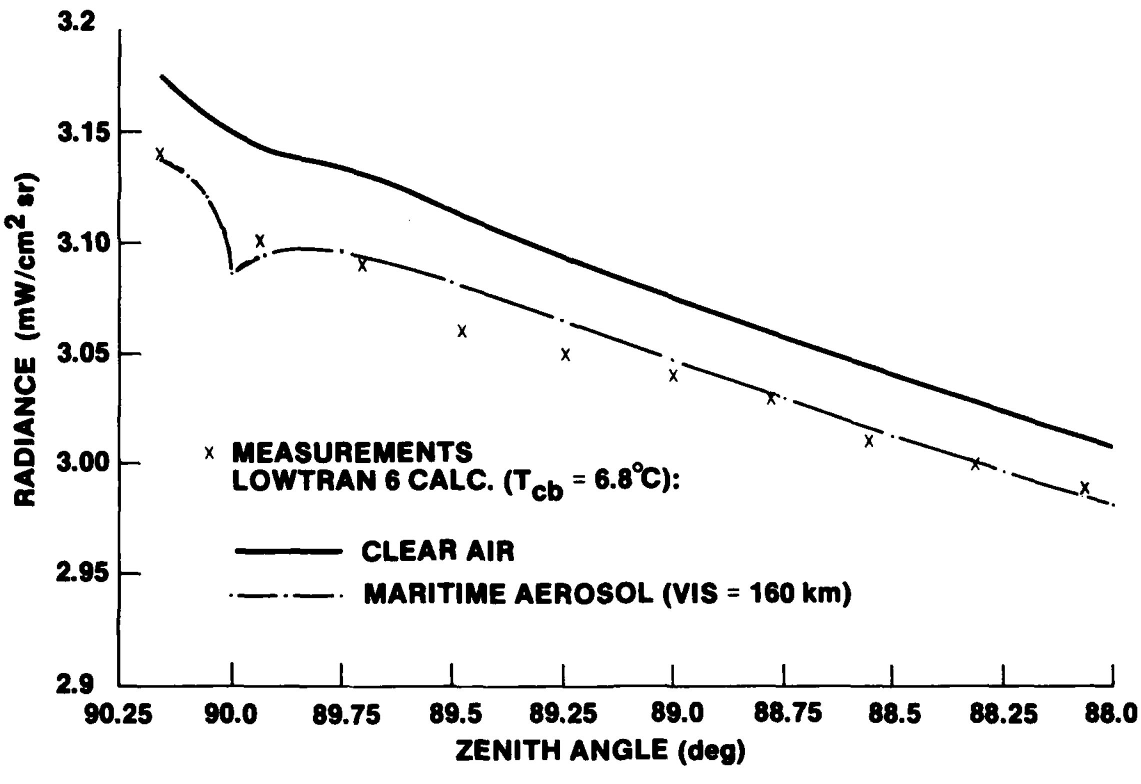

Figure 4. Comparison of measured and calculated infrared (8–12 μm) sky radiances versus zenith angle and for overcast sky conditions (15 April 1986, 1945 PST).

(Hughes and Thompson, 1984). The clear-air radiance calculations are slightly greater than the measured values, indicating a small presence of aerosols, i.e., a scattering loss of radiation. The measured and calculated values can be brought into good agreement by including either the LOWTRAN Maritime Model (visibility = 160 km) or the Urban Model (visibility = 100 km). This demonstrates that aerosol size distributions inferred via this method are not necessarily unique. Uniqueness, however, is not a requirement in specifying atmospheric optical depths. Without including the boundary temperature, calculated radiances (with or without aerosols) at 88° zenith angle are approximately 10% lower than shown in the figure. In contrast, the calculated radiances at the horizon (zenith angle = 98.16° in this case) are insensitive to the cloud boundary due to the low atmospheric transmittance over the path lengths contributing to the sky radiance. This is demonstrated in Fig. 5, in which the horizon radiance is calculated with and without the cloud-base temperature and by varying the cloud-base altitude, its temperature, and the number of radiosonde levels. Utilizing only the first two levels of the radiosonde data (assuming the cloud base at 143 m), the radiances calculated with and without the boundary temperature differ by less than 1%.

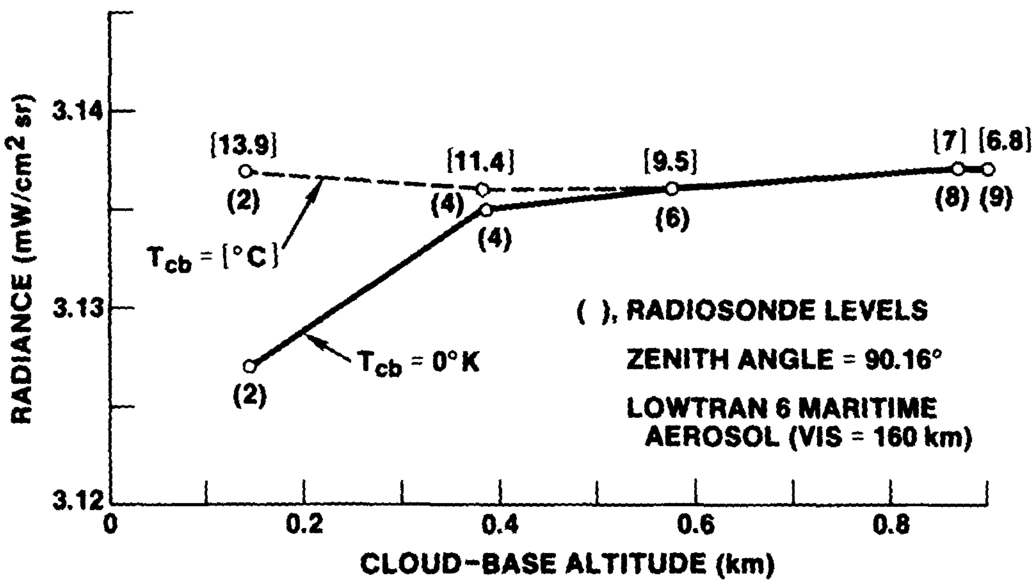

Figure 5. Infrared (8-12 μm) horizon radiances calculated with and without the cloud-base temperature and by varying cloud-base altitude, its temperature, and the number of radiosonde levels (15 April 1986).

An important feature of the radiance calculated with aerosols in Fig. 4 is the dip occurring at 90°. This dip is found to occur when even the slightest contributions of aerosols are included in the LOWTRAN calculations. This is further evident in Fig. 6, where the sky radiances (data of third radiosonde launch) measured with zenith angle are compared with the LOWTRAN calculations. As for the previous case, the measurements are lower than the clear-air calculations. By including aerosols (Maritime Model with a visibility of 70 km), the calculated radiance can be made to agree with the measurements at the optical horizon (zenith angle = 90.17°). As the zenith angle is decreased, the calculated radiances depart from the measurements and approach the clear-air calculations. This discrepancy may result from an inappropriate vertical lapse rate in the aerosol model or contamination of the measured radiances by the scattered stratus clouds present at the time. (These scattered cloud conditions do not allow a cloud-base temperature to be defined as in the previous case.) In Fig. 6, the dip in radiance occurring at 90° zenith angle is seen to be sensitive to the number of radiosonde levels below 1 km included in the LOWTRAN calculations. This dip in calculated radiance is most likely an artifact (yet to be determined) of the LOWTRAN ray trace technique. In contrast, the radiance at the horizon can be calculated to within 98.6% of the measured value using only one atmospheric layer (two radiosonde levels). This is demonstrated in Fig. 7, where the

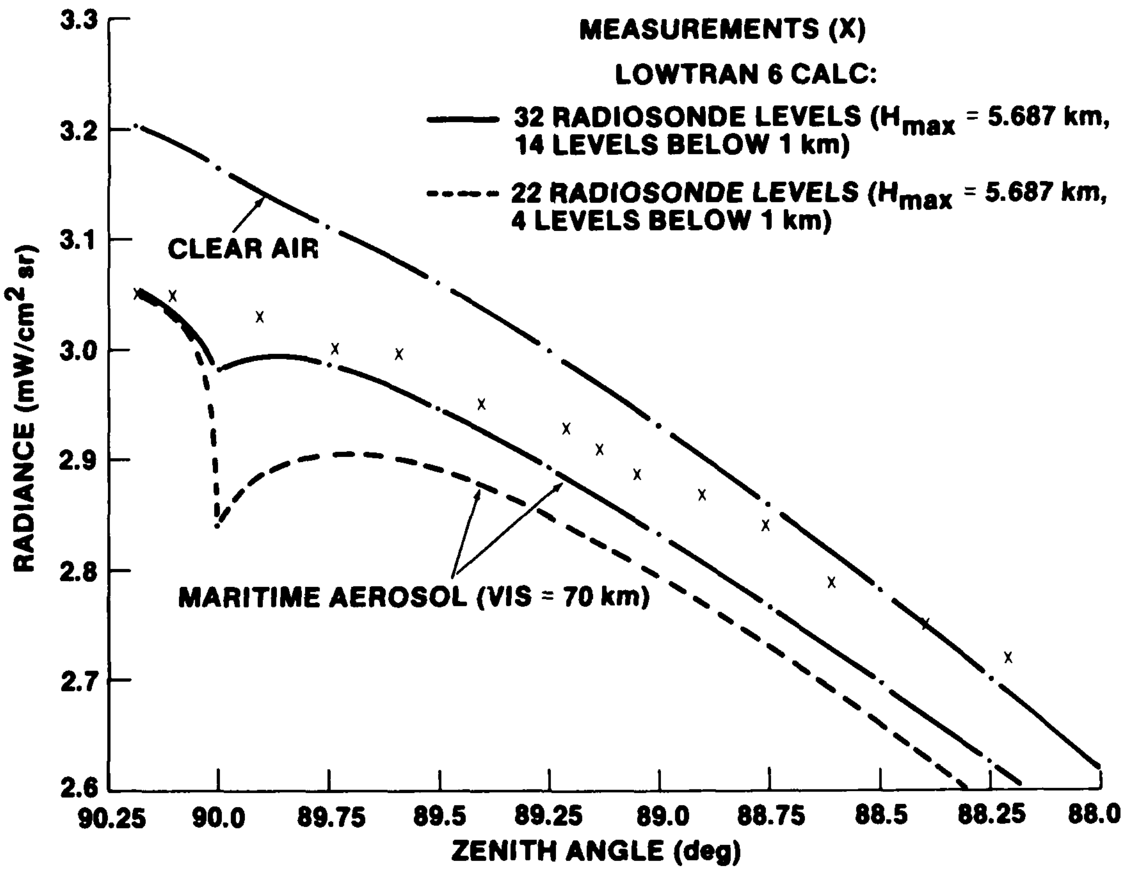

Figure 6. Comparison of measured and calculated infrared (8-12 μm) sky radiances versus zenith angle for scattered cloud conditions (16 April 1986, 1245 PST).

horizon radiance is calculated by varying the maximum altitude and number of levels in the radiosonde inputs. These data raise serious questions about the LOWTRAN radiance algorithm. It has been proposed by others (Ben-Shalom, et al., 1980) that the LOWTRAN algorithm was deficient in that multiple-scattering effects over the long propagation paths were not properly addressed. However, utilizing similar data (as in the present report), it has been shown (Hughes, et al., 1986) that the multiple-scattering modifications to LOWTRAN proposed by Ben-Shalom do not explain the radiance dip at 90° and grossly

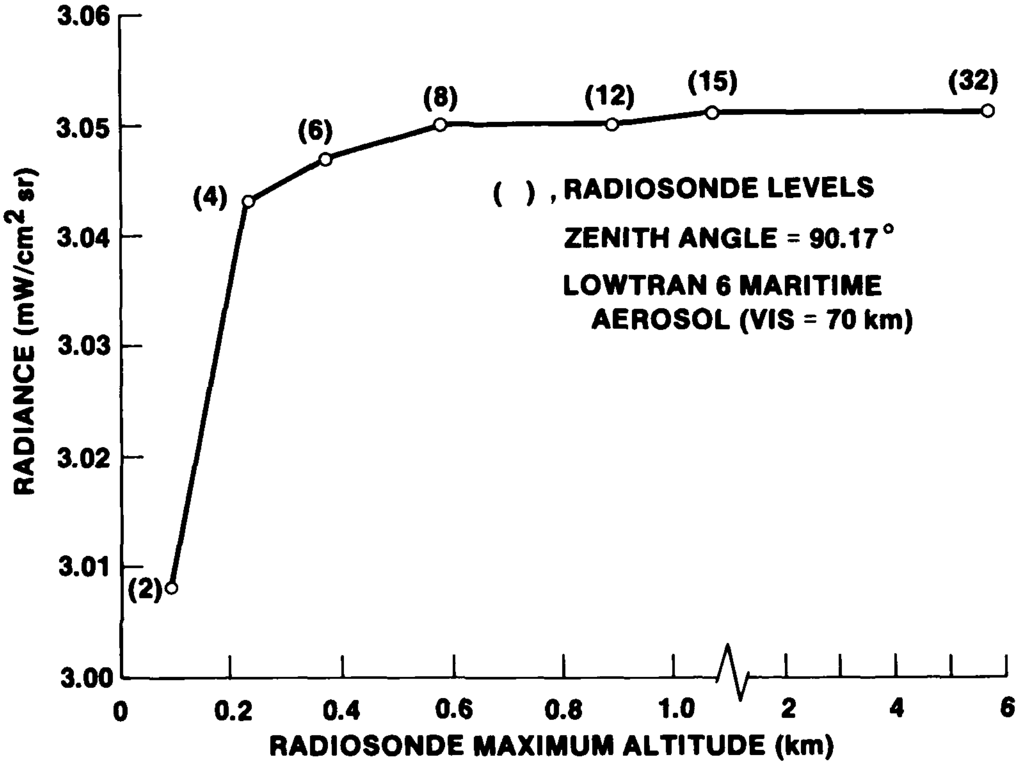

Figure 7. Infrared (8-12 μm) horizon radiances calculated by varying the maximum altitude and number of radiosonde levels (16 April 1986).

overestimate the horizon sky radiances when aerosols are present. With these uncertainties, we are left with considering only the radiance comparisons at the optical horizon. Table 2 lists the measured horizon radiances and those calculated by means of three current LOWTRAN 6 aerosol models (Maritime, Urban,and Navy Maritime). The clear-air calculations were made using plus and minus uncertainties (0.5°C in temperature and 5% in relative humidity) in the radiosonde measurements. With the exception of the minus uncertainty for the first radiosonde launch (4/15/86), the clear-air radiances due to the uncertainty were greater than the measurements indicating a *small* presence of aerosols. By adjusting the surface visibility, the radiances calculated via each model can be made to agree closely with the measured value. For the Navy Maritime Model, the calculations were made with an air mass factor of unity for maritime air and the 24-hour average and current surface wind speeds shown in Fig. 2. The very high surface visibility requirements needed to bring the calculated and measured radiances into agreement stem from the instantaneous wind speed component of the model, which causes the aerosol scattering coefficients to be grossly overestimated.

Table 2. Comparisons of measured infrared (8–12 μm) horizon radiances (mW/cm^{2}sr) with those calculated for clear-air conditions and with three current LOWTRAN aerosol models.

(time) (date)	1945 PST 4/15/86	0845 PST 4/16/86	1245 PST 4/16/86	1645 PST 4/16/86
MEASUREMENTS	3.14±.01	3.10 ±.01	3.05±.01	3.06±.01
LOWTRAN 6 CALC:				
CLEAR AIR	$3.173^{+.029}_{-.027}$	$3.198^{+.028}_{-.027}$	$3.201^{+.031}_{-.032}$	$3.211^{+.031}_{-.034}$
MARITIME (VIS = 160 km)	3.137			
(VIS = 70 km)		3.082	3.051	3.061
URBAN (VIS = 100 km)	3.137			
(VIS = 35 km)		3.092	3.058	3.068
NAVY MARITIME	*			
(VIS = 130 km)		3.101		
(VIS = 210 km)			3.052	
(VIS = 210 km)				3.059

* 24-HOUR AVG. WIND SPEED NOT AVAILABLE
(VIS) = SURFACE METEOROLOGICAL RANGE

DISCUSSION

This investigation has demonstrated that infrared (8–12 μm) horizon sky radiances can be adequately modeled by the LOWTRAN 6 computer code, using the meteorological parameters in the first 100 to 200 m of the atmosphere. Also, clouds do not contribute to the horizon radiance but must be properly included in LOWTRAN calculations at other altitudes. These results also indicate that an appropriate aerosol model for transmittance calculations can be inferred from vertical measurements of meteorological parameters and horizon radiances. However, a deficiency in the LOWTRAN radiance (and transmittance) algorithm at a zenith angle of $90° \pm 0.1°$ was pointed out. This discrepancy (which is not related to the neglect of multiple-scattering effects, at least for this wavelength band), must be accounted for if meaningful interpretations of aerosol effects on sky radiance measurements can be made.

An alternative approach to infer an appropriate aerosol size distribution from radiance measurements is to utilize the sun as a source at other wavelengths (near- and mid-IR), which are affected by atmospheric aerosols at zenith angles less than 80°, where the LOWTRAN "layering" anomaly is not important. This is demonstrated in Fig. 8, in which the solar radiance (calculated by LOWTRAN 6) received near the ground (H_1 = 33 m) is plotted versus the air mass factor, sec θ, where θ is the solar zenith angle. The 1962 standard atmosphere was used in the clear-air calculations and with the Maritime Aerosol Model for differing visibilities. The calculations apply to the near-IR (1.33–1.67 μm) and mid-IR (3–5 μm) bands. For visibilities less than 23 km and zenith angles between 60° and 80°, the differences between the clear-air calculations and those with aerosols are well within the measuring capabilities of currently available radiometer systems. This technique, however, would be limited to the daytime and cloud-free lines-of-sight. Yet to be determined is how effective the size distributions determined by the shorter wavelength bands would be in predicting transmittances at far-IR bands.

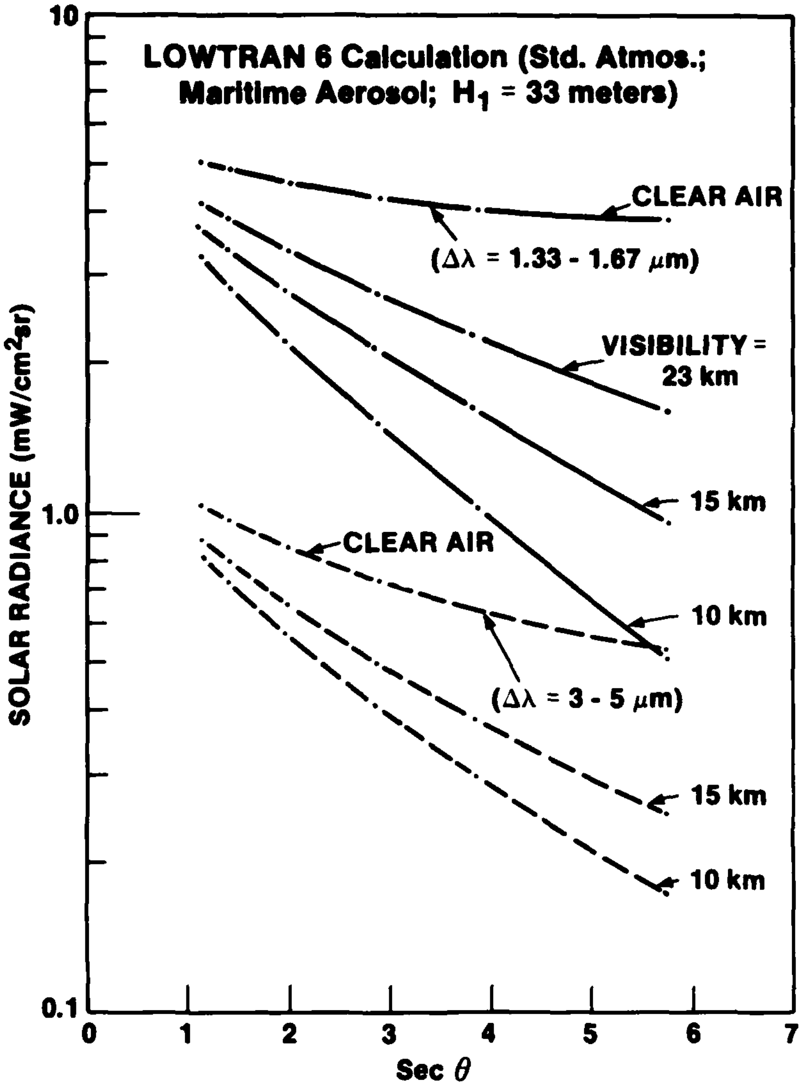

Figure 8. Calculated solar radiances received near the ground versus the air mass factor for near- and mid-IR wavelengths for differing visibilities.

REFERENCES

Ben-Shalom, A., B. Barzilia, D. Cabib, A. D. Devir, S. G. Lipson, and U. P. Oppenheim, "Sky Radiance at Wavelengths Between 7 and 14 μm: Measurement, Calculation, and Comparison with LOWTRAN-4 Predictions," Appl. Opt., 19, 838 (1980).

Hughes, H. G., W. J. Schade, and L. R. Hitney, "Effects of Aerosols on Low-Elevation Infrared Sky Radiances," Appl. Opt., 25, 1536 (1986).

Hughes, H. G., and B. L. Thompson, "Estimates of Optical Pulse Broadening in Maritime Stratus Clouds," Opt. Eng., 23, 38, 1984.

Kneizys, F. X., et al., "Atmospheric Transmission/Radiance: Computer Code LOWTRAN 6," AFGL-TR-83-0187 (1983).

Schade, W. J., and D. B. Law, "Infrared Sky Radiance Distributions in the Marine Boundary Layer," NOSC Technical Document 1032, 1986.

Stephens, G. L., "Radiation Profiles in Extended Water Clouds. II: Parameterization Schemes," J. Atmos. Sci., 35, 2123 (1978).

END
2-87
DTIC